

# GSA DATA REPOSITORY 2015223

## Hydrological changes facilitated early rice farming in the lower Yangtze River Valley in China: A molecular isotope analysis

Robert Patalano<sup>1</sup>, Zheng Wang<sup>2</sup>, Qin Leng<sup>1</sup>, Weiguo Liu<sup>2</sup>, Yunfei Zheng<sup>3</sup>, Guoping Sun<sup>3</sup>, and Hong Yang<sup>1\*</sup>

<sup>1</sup>Laboratory for Terrestrial Environments, Department of Science and Technology, College of Arts and Sciences, Bryant University, 1150 Douglas Pike, Smithfield, RI 02917, U.S.A.

<sup>2</sup>State Key Laboratory of Loess and Quaternary Geology, Institute of Earth Environment, Chinese Academy of Science, 97 Yanxiang Road, Xi'an, 710061, P.R. China

<sup>3</sup>Zhejiang Province Institute of Archeology and Cultural Heritage, Hangzhou, 310014, P.R. China

\* Corresponding author: 401 232 6223; Email: [hyang@bryant.edu](mailto:hyang@bryant.edu)

## THE TIANLUOSHAN ARCHEOLOGICAL SITE AND CHRONOLOGY

- The Tianluoshan archaeological site was discovered in 2001 and was recognized to be a representative of the Neolithic Hemudu Culture, with the Early and the Late Cultural Periods dating to 7.0-6.0 Ka and 6.0-5.5 Ka (Li and Sun, 2009; Sun, 2009; Sun, 2011; Zheng, et al., 2009, 2012; Zhejiang Province Institute of Archaeology and Cultural Heritage et al., 2007).
- Chronology was calibrated by IntCal 13 (Reimer et al., 2013) using the OxCal v4.2.3 software (Bronk Ramsey, 2013) (Fig. DR1 and Table DR1). As the bottom of the sequence was not constrained by radiometric dates, we calculated the ages for bottom of Layers 12 and 13 based upon an average sedimentation rate (0.0885 cm/year) calculated using the radiometric dated age model.

## EXTENDED METHOD FOR MOLECULAR $\delta^{13}\text{C}$ and $\delta\text{D}$ MEASUREMENTS

Among the thirteen layers, the topmost layer (Layer 1) corresponding to the modern rice paddy field was not analyzed in this study.

- Sedimentary samples were lyophilized using a Labconco FreeZone 4.5 Liter Console Freeze Dry System.
- Total lipid extraction (TLE) extracted using a Dionex 350 Accelerated Solvent Extraction (ASE) at 125°C and 1500-1600 p.s.i. for 26 min with a dichloromethane:methanol = 2:1 (v/v) buffer.
- Gas chromatography (GC) analysis was performed using an Agilent 6890 Series with HP1-ms GC column (60 m length, 0.32 mm i.d. and 0.25  $\mu\text{m}$  film) with flame ionization detector (FID). Fifty-six of the 63 extracted sedimentary samples yielded sufficient quantity of n-alkanes for both carbon and hydrogen isotope measurements.
- Peak areas for *n*-alkanes compared with an external standard mixture ( $\text{C}_{21}$ – $\text{C}_{33}$ , odd carbon numbers) (Fig. DR2).

- $\delta^{13}\text{C}$  and  $\delta\text{D}$  expressed relative to the VPDB and VSMOW defined as the following:  $\delta^{13}\text{C} = 1000 \times [(\text{sample}/^{12}\text{C}_{\text{sample}})/(\text{VPDB}/^{12}\text{C}_{\text{VPDB}}) - 1]$ ;  $\delta\text{D} = 1000 \times [^2\text{H}/^1\text{H}_{\text{sample}}/^2\text{H}/^1\text{H}_{\text{VSMOW}} - 1]$ .

## DETAILED CARBON AND HYDROGEN ISOTOPE DATA

- Molecular carbon isotopic values of extracted *n*-alkanes range from -33.1‰ to -27.9‰ for C<sub>27</sub>, -35.9‰ to -29.3‰ for C<sub>29</sub>, and -38‰ to -29.7‰ for C<sub>31</sub>; the average  $\delta^{13}\text{C}$  values of long-chain *n*-alkanes from the three *n*-alkane molecules vary from -35‰ to -29.2‰.
- Molecular hydrogen isotopic values of extracted *n*-alkanes range from -207‰ to -107‰ for C<sub>27</sub>, -209‰ to -126‰ for C<sub>29</sub>, and -205‰ to -125‰ for C<sub>31</sub>; the average  $\delta\text{D}$  values of long-chain *n*-alkanes from the three compounds vary from -207‰ to -123‰ in the recorded section.
- Detailed measurements of  $\delta^{13}\text{C}$  and  $\delta\text{D}$  values of individual compounds along the T705 sequence is tabulated in Table DR2 with graphic representation presented in Fig. DR3, along with calculated averaged values, standard deviation, sequence depth, and carbon age.

## DATA REPOSITORY (DR) TABLES AND FIGURES

Depth (cm)	<sup>14</sup> C Age BP	Range (Cal. Age BP)	Median (Cal. Age BP)	Error ( $\pm 2\sigma$ )
62.5	1990±40	2043-1832	1937.5	105.5
82.5	4020±40	4782-4414	4598	184
92.5	4275±40	4962-4708	4835	127
117.5	4585±35	5450-5061	5255.5	194.5
132.5	4660±40	5573-5309	5441	132
177.5	5465±45	6394-6184	6289	105
252.5	5620±35	6474-6311	6392.5	81.5
292.5	6120±45	7160-6893	7026.5	133.5

**Table DR1.** Chronological calibration of the south section of T705 profile at Tianluoshan site by IntCal 13 at 95.4% probability or 2 standard deviations ( $\sigma$ ).

Layer	Sampling number	Depth (cm)	$\delta^{13}\text{C}_{\text{C}_{27}}$	$\delta^{13}\text{C}_{\text{C}_{29}}$	$\delta^{13}\text{C}_{\text{C}_{31}}$	$\delta^{13}\text{C}$ Average	Standard deviation	$\delta\text{D}_{\text{C}_{27}}$	$\delta\text{D}_{\text{C}_{29}}$	$\delta\text{D}_{\text{C}_{31}}$	$\delta\text{D}$ Average	Standard deviation	$^{14}\text{C}$ Age BP
3	#-6	45-50	-28.6	-29.3	-29.7	-29.2	0.6	-117	-135	-149	-133.7	16.0	
	#-5	50-55	-28.2	-29.5	-30.9	-29.5	1.4	-122	-175	-151	-149.3	26.5	
	#-4	55-60	N.D.	N.D.	N.D.	N.D.	N.D.	N.D.	N.D.	N.D.	N.D.	N.D.	
	#-3	60-65	-31.0	-32.9	-35.4	-33.1	2.2	-182	-199	-194	-191.7	8.7	1990±40
	#-2	65-70	-31.1	-33.5	-35.5	-33.4	2.2	-186	-200	-192	-192.7	7.0	
	#-1	70-75	-30.8	-32.2	-36.5	-33.2	3.0	-174	-196	-187	-185.7	11.1	
	#0	75-80	-31.5	-33.1	-35.5	-33.4	2.0	-184	-200	-194	-192.7	8.1	
4	#1	80-85	-32.7	-34.7	-35.6	-34.3	1.5	-189	-201	-198	-196.0	6.2	4020±40
	#2	85-90	-32.1	-32.9	-34.1	-33.0	1.0	-188	-201	-195	-194.7	6.5	
4/5	#3	90-95	-31.5	-33.4	-35.4	-33.4	2.0	-197	-198	-195	-196.7	1.5	4275±40
5	#4	95-100	-30.8	-32.0	-33.6	-32.1	1.4	-200	-200	-196	-198.7	2.3	
	#5	100-105	-30.6	-32.0	-33.6	-32.1	1.5	-206	-206	-200	-204.0	3.5	
	#6	105-110	-31.0	-32.6	-34.2	-32.6	1.6	-204	-205	-199	-202.7	3.2	
	#7	110-115	-30.6	-31.5	-33.5	-31.9	1.5	-198	-200	-196	-198.0	2.0	
5/6	#8	115-120	-31.1	-32.0	-33.5	-32.2	1.2	-196	-199	-195	-196.7	2.1	4585±35
6	#9	120-125	-31.1	-32.2	-33.0	-32.1	1.0	-194	-200	-196	-196.7	3.1	
	#10	125-130	-31.3	N.D.	N.D.	-31.3	N.D.	N.D.	N.D.	N.D.	N.D.	N.D.	
6/7	#11	130-135	-31.2	-32.7	-33.9	-32.6	1.4	-207	-207	-201	-205.0	3.5	4660±40
7	#12	135-140	-30.5	-32.3	-33.8	-32.2	1.7	-201	-201	-201	-201.0	0.0	
	#13	140-145	-31.5	-32.9	-34.1	-32.8	1.3	-207	-209	-205	-207.0	2.0	
	#14	145-150	-30.8	-32.7	-34.6	-32.7	1.9	-204	-206	-201	-203.7	2.5	
	#15	150-155	-32.5	-33.1	-33.3	-33.0	0.4	-204	-203	-197	-201.3	3.8	
	#16	155-160	-31.6	-32.1	N.D.	-31.9	0.4	N.D.	N.D.	N.D.	N.D.	N.D.	
	#17	160-165	-32.0	-32.9	-34.3	-33.1	1.2	-203	-198	-194	-198.3	4.5	
	#18	165-170	-31.5	-33.4	-34.4	-33.1	1.5	-191	-189	-190	-190.0	1.0	
	#19	170-175	-30.9	-32.5	-34.6	-32.7	1.9	-193	-197	-195	-195.0	2.0	
7/8	#20	175-180	-30.1	-33.9	-34.7	-32.9	2.5	-179	-189	-187	-185.0	5.3	5465±45
8	#21	180-185	-30.2	-35.2	-34.4	-33.3	2.7	N.D.	N.D.	N.D.	N.D.	N.D.	
	#22	185-190	-31.4	-31.4	-32.9	-31.9	0.9	-155	-177	-170	-167.3	11.2	
	#23	190-195	-28.9	-30.0	-31.3	-30.1	1.2	-114	-144	-153	-137.0	20.4	
	#24	195-200	-31.1	-31.8	-33.2	-32.0	1.1	-142	-150	-157	-149.7	7.5	
	#25	200-205	-29.3	-33.4	-34.9	-32.5	2.9	-109	-150	-169	-142.7	30.7	
	#26	205-210	-30.6	-31.5	-32.8	-31.6	1.1	N.D.	N.D.	N.D.	N.D.	N.D.	
	#27	210-215	-31.5	-34.9	-34.0	-33.5	1.8	N.D.	N.D.	N.D.	N.D.	N.D.	
	#28	215-220	-31.5	-33.6	-33.5	-32.9	1.2	N.D.	N.D.	N.D.	N.D.	N.D.	
	#29	220-225	N.D.	-33.6	-36.4	-35.0	2.0	N.D.	N.D.	N.D.	N.D.	N.D.	
	#30	225-230	-30.9	-32.3	-33.3	-32.2	1.2	-168	-178	-182	-176.0	7.2	
	#31	230-235	-30.9	-32.6	-37.1	-33.5	3.2	N.D.	N.D.	N.D.	N.D.	N.D.	
	#32	235-240	-31.7	-35.9	-35.7	-34.4	2.4	N.D.	N.D.	N.D.	N.D.	N.D.	

	#33	240-245	-31.0	-33.4	-35.9	-33.4	2.5	-161	-189	-190	-180.0	16.5	
	#34	245-250	N.D.	N.D.	N.D.	N.D.	N.D.	N.D.	N.D.	N.D.	N.D.	N.D.	
8/9	#35	250-255	-33.1	-35.7	-36.2	-35.0	1.7	-195	-196	-198	-196.3	1.5	5620±35
9	#36	255-260	-33.0	-34.4	-36.1	-34.5	1.6	-187	-191	-193	-190.3	3.1	
	#37	260-265	-32.1	-33.4	-35.3	-33.6	1.6	-190	-196	-190	-192.0	3.5	
10	#38	265-270	-31.9	-34.1	-35.7	-33.9	1.9	-192	-191	-188	-190.3	2.1	
	#39	270-275	-32.1	-33.9	-35.4	-33.8	1.7	-182	-192	-192	-188.7	5.8	
10/11	#40	275-280	-31.9	-33.6	-35.6	-33.7	1.9	-180	-191	-185	-185.3	5.5	
11	#41	280-285	-31.6	-32.8	-35.6	-33.3	2.1	-186	-192	-189	-189.0	3.0	
	#42	285-290	-30.8	-32.6	-35.5	-33.0	2.4	-183	-187	-178	-182.7	4.5	
11/12	#43	290-295	-31.1	-32.1	-33.7	-32.3	1.3	-135	-152	-151	-146.0	9.5	6120±45
12	#44	295-300	-29.4	-30.3	-34.2	-31.3	2.6	-138	-143	-142	-141.0	2.6	
	#45	300-305	-30.3	-33.7	-37.3	-33.8	3.5	-151	-176	-168	-165.0	12.8	
	#46	305-310	-30.6	-33.7	-38.0	-34.1	3.7	-170	-188	-181	-179.7	9.1	
	#47	310-315	N.D.	N.D.	N.D.	N.D.	N.D.	N.D.	N.D.	N.D.	N.D.	N.D.	
12/13	#48	315-(319)320 320-325	-29.2	-31.7	-33.6	-31.5	2.2	-144	-167	-164	-158.3	12.5	
13	#49		-29.7	-32.5	-34.8	-32.3	2.6	N.D.	N.D.	N.D.	N.D.	N.D.	
	#50	325-330	N.D.	N.D.	N.D.	N.D.	N.D.	N.D.	N.D.	N.D.	N.D.	N.D.	
	#51	330-335	-28.9	-30.4	-31.7	-30.3	1.4	N.D.	N.D.	N.D.	N.D.	N.D.	
	#52	335-340	-29.0	-29.5	-32.8	-30.4	2.1	N.D.	N.D.	N.D.	N.D.	N.D.	
	#53	340-345	-28.3	-29.7	-35.7	-31.2	3.9	N.D.	N.D.	N.D.	N.D.	N.D.	
	#54	345-350	-28.4	-29.8	-32.4	-30.2	2.0	-113	-142	-153	-136.0	20.7	
	#55	350-355	-27.9	-29.8	-33.2	-30.3	2.7	-120	-126	-125	-123.7	3.2	
	#56	355-360	N.D.	N.D.	N.D.	N.D.	N.D.	-107	-155	-161	-141.0	29.6	

**Table DR2.** Database for measured molecular C and H isotope from T705 profile at Tianluoshan site.

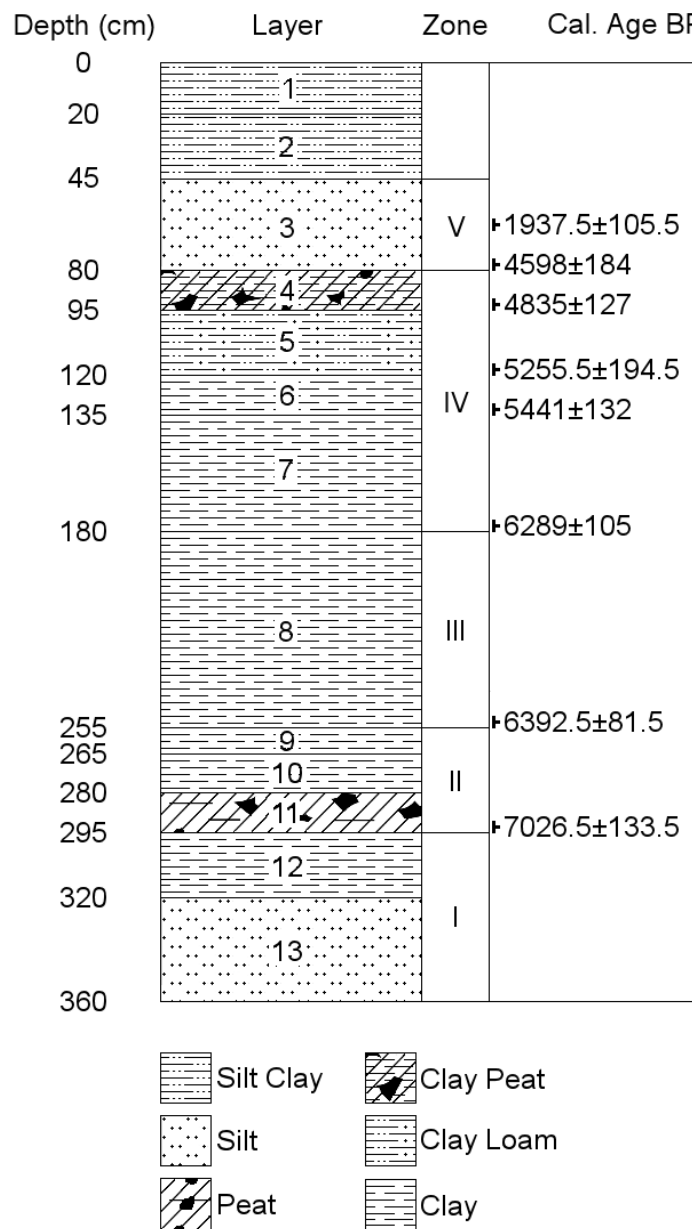


**Fig. DR1.** Lithology, reconstructed ecological zones (Zheng et al., 2012), and chronology of T705 profile at Tianluoshan site. Zones II and IV contains domesticated rice remains known as the early rice layer and the late rice layer respectively.

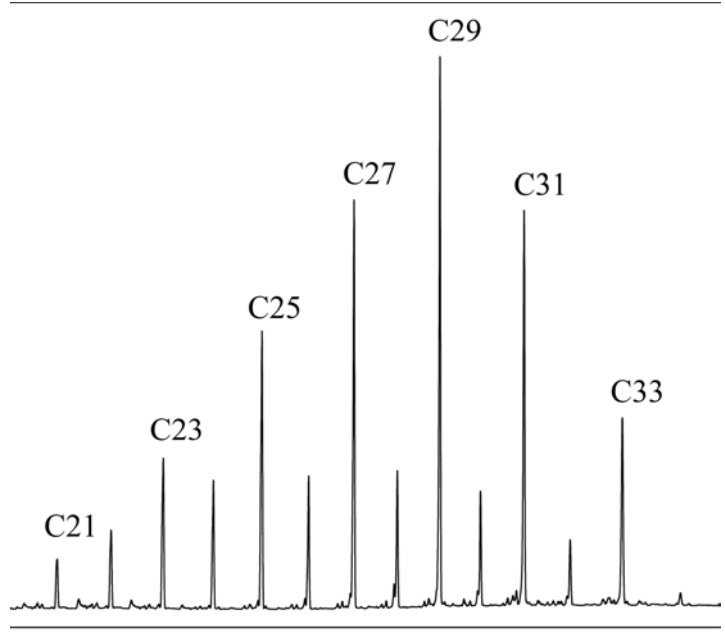


**Fig. DR2.** GC-FID trace of a typical *n*-alkane distribution of T705 profile sediments (#37, 260-265cm) at Tianluoshan site, showing C<sub>29</sub> dominating *n*-alkane profile, typical from terrestrial higher plants.

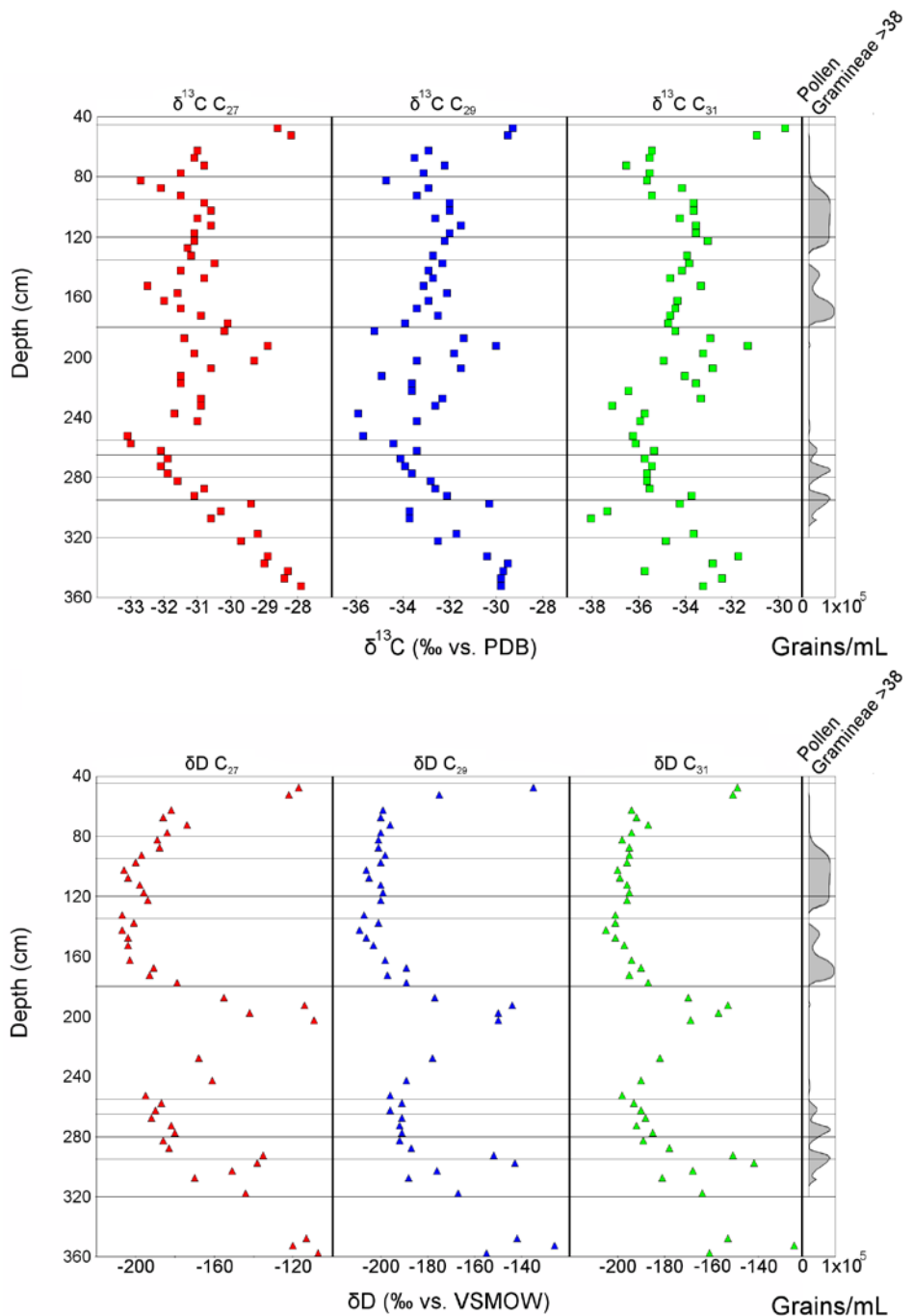


**Fig. DR3.** Molecular  $\delta^{13}\text{C}$  (upper panel) and  $\delta\text{D}$  (lower panel) values from three compounds (C<sub>27</sub>-C<sub>31</sub>) *n*-alkanes of T705 profile at Tianluoshan site were plotted against sequence depth and grass pollen diagram from a nearby T1041 profile (Zheng et al. 2009). Horizontal lines indicate stratigraphic layers. Although some of the samples did not yield a measurable quantity of *n*-alkanes for isotope measurement, trends in both carbon and hydrogen isotope values and correlations between values of the two stable isotopes are clearly recorded along the sequence.

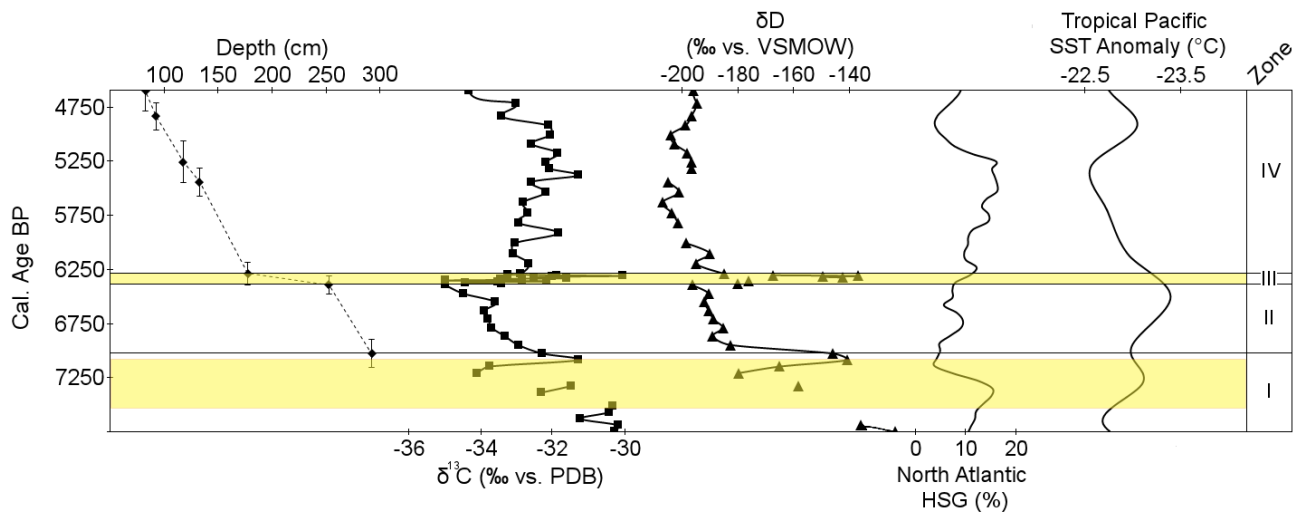


**Fig. DR4.** Comparison of high-resolution *n*-alkane carbon and hydrogen isotope record of the Tianluoshan area with SST curve from tropical Pacific anomalies (Koutavas et al., 2006; Koutavas and Joanides, 2012) and hematite-stained grain (HSG) records, expressed as percentages of lithic grains (ice-raftered debris, IRD), from the North Atlantic (Bond et al., 2001), between 7.2 Ka and 4.6 Ka, under our depth-age model in text Fig 3.

## DR REFERENCES

- Bronk Ramsey, C., & Lee, S., 2013, Recent and Planned Developments of the Program OxCal. Radiocarbon, 55(2-3), 720-730.
- Innes, J. B., Zong, Y., Chen, Z., Chen, C., Wang, Z., and Wang, H., 2009, Environmental history, palaeoecology and human activity at the early Neolithic forager/cultivator site at Kuahuqiao, Hangzhou, eastern China: Quaternary Science Reviews, v. 28, no. 23-24, p. 2277-2294.
- Koutavas, A., deMenocal, P. B., Olive, G. C., and Lynch-Stieglitz, J., 2006, Mid-Holocene El Niño–Southern Oscillation (ENSO) attenuation revealed by individual foraminifera in eastern tropical Pacific sediments: Geology, v. 34, no. 12, p. 993-996.
- Koutavas, A., and Joanides, S., 2012, El Niño–Southern Oscillation extrema in the Holocene and Last Glacial Maximum: Paleoceanography, v. 27, no. 4.
- Li, A.-J., Sun, G.-P., 2009. Tianluoshan Site, a new window of Hemudu Culture, Xiling Seal Society Publishing House, Hangzhou, 240 pp. (in Chinese with English abstract)

- Reimer, P. J., Bard, E., Bayliss, A., Beck, J. W., Blackwell, P. G., Ramsey, C. B., Buck, C. E., Cheng, H., Edwards, R. L., Friedrich, M., Grootes, P. M., Guilderson, T. P., Haflidason, H., Hajdas, I., Hatté, C., Heaton, T. J., Hoffmann, D. L., Hogg, A. G., Hughen, K. A., Kaiser, K. F., Kromer, B., Manning, S. W., Niu, M., Reimer, R. W., Richards, D. A., Scott, E. M., Southon, J. R., Staff, R. A., Turney, C. S. M., and van der Plicht, J., 2013, IntCal13 and Marine13 Radiocarbon Age Calibration Curves 0-50,000 Years Cal BP: Radiocarbon, v. 55, no. 4, p. 1869-1887.
- Sun, G.-P., 2009. Tianluoshan Site, a New Window of Hemudu Culture (Editor-in-Chief Li. An-Jun). Xiling Seal Society Publishing House, Hangzhou (in both Chinese and English).
- Sun, G.-P., 2011. Preliminary report of the first stage (2004-2008) archaeological excavation of Tianluoshan Site, In: Center for the Study of Chinese Archaeology, Peking University & Zhejiang Province Institute of Archaeology and Cultural Heritage (Eds.) Integrated studies on the natural remains from Tianluoshan., Cultural Relics Press, Beijing, pp. 7-39 (in Chinese with English title).
- Yang, H., and Huang, Y.-S., 2003, Preservation of lipid hydrogen isotope ratios in Miocene lacustrine sediments and plant fossils at Clarkia, northern Idaho, USA: Organic Geochemistry, p. 413-423.
- Zhejiang Province Institute of Relics and Archaeology, et al., 2007, Brief Report of the Excavation on a Neolithic Site at Tianluoshan Hill in Yuyao, Zhejiang, Chinese, vol. 11. Cultural Relics, pp. 4-24. (in Chinese with English abstract)
- Zheng, Y.-F., Sun, G.-P., Qin, L., Li, C.-H., Wu, X.-G., 2009. Rice fields and modes of rice cultivation between 5000 and 2500 BC in east China, Journal of Archaeological Science 36, 2609-2616.
- Zheng, Y.-F., Sun, G.-P., and Chen, X.-G., 2012, Response of rice cultivation to fluctuating sea level during the Mid-Holocene: Chinese Science Bulletin, v. 57, no. 4, p. 370-378.